A micro-chip initiator with controlled combustion reactivity realized by integrating Al/CuO nanothermite composites on a microhotplate platform

2016 J. Micromech. Microeng. 26 015002

(http://iopscience.iop.org/0960-1317/26/1/015002)

IOP Publishing Journal of Micromechanics and Microengineering
J. Micromech. Microeng. **26** (2016) 015002 (10pp) doi:10.1088/0960-1317/26/1/015002

A micro-chip initiator with controlled combustion reactivity realized by integrating Al/CuO nanothermite composites on a microhotplate platform

Ji Young Ahn[1], Sang Beom Kim[2], Ji Hoon Kim[2], Nam Su Jang[2], Dae Hyun Kim[3], Hyung Woo Lee[1,2,4], Jong Man Kim[1,2,4] and Soo Hyung Kim[1,2,4]

[1] Research Center for Energy Convergence Technology, Pusan National University, 30 Jangjeon-dong, Geumjung-gu, Busan 609–735, Korea
[2] Department of Nano Fusion Technology, Pusan National University, 30 Jangjeon-dong, Geumjung-gu, Busan 609–735, Korea
[3] Copper Business Unit, Poongsan Holdings Corporation, 670 Gongdan-ro, Seongsan-gu, Chang Won, Gyeong Nam 642-120, Korea
[4] Department of Nano Energy Engineering, Pusan National University, 30 Jangjeon-dong, Geumjung-gu, Busan 609–735, Korea

E-mail: sookim@pusan.ac.kr and jongkim@pusan.ac.kr

Received 11 July 2015, revised 6 October 2015
Accepted for publication 20 October 2015
Published 26 November 2015

Abstract

The interfacial contact area between the fuel and oxidizer components plays an important role in determining the combustion reactivity of nanothermite composites. In addition, the development of compact and reliable ignition methods can extend the applicability of nanothermite composites to various thermal engineering fields. In this study we report the development of a micro-chip initiator with controlled combustion reactivity using concepts usually applied to microelectromechanical systems (MEMS) and simple nanofabrication processes. The nanothermite composites fabricated in this study consisted of aluminum nanoparticles (Al NPs) as the fuel and copper oxide nanoparticles (CuO NPs) as the oxidizer accumulated on a silicon oxide substrate with a serpentine-shaped gold (Au) electrode. The micro-chip initiator rapidly ignited and exploded when minimal current was supplied. The effects of stacking structures of Al and CuO-based multilayers on the combustion properties were systematically investigated in terms of the pressurization rate, peak explosion time, and heat flow. Pressurization rates of 0.004–0.025 MPa μs^{-1} and heat flows of 2.0–3.8 kJ g^{-1} with a commonly fast response time of less than 20 ms could be achieved by simply changing the interfacial structures of the Al and CuO multilayers. The controllability of combustion reactivity of micro-chip initiator can be made for general nanothermite composites composed of Al and various metal oxides (e.g. Fe_2O_3, CuO, $KMnO_4$, etc). The micro-chip initiator fabricated in this study was reliable, compact, and proved to be a versatile platform, exhibiting controlled combustion reactivity and fast response time, which could be used for various civilian and military thermal engineering applications, such as in initiators and propulsion, welding, and ordinance systems.

Keywords: nanothermite composites, microelectromechanical process, aluminum, copper oxide, ignition, combustion property

(Some figures may appear in colour only in the online journal)

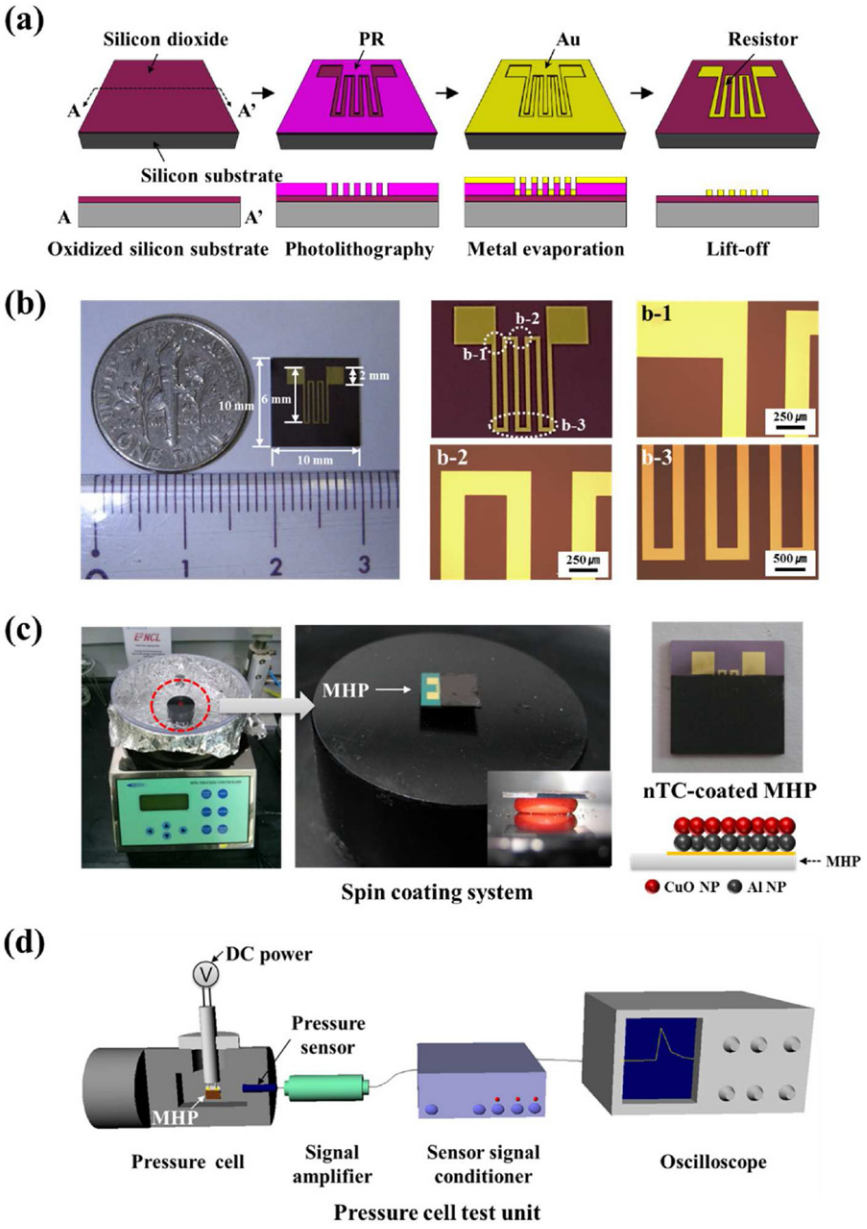

Figure 1. (a) The schematic representation of the MEMS-based processes used for fabricating the MHPs, (b) photographs and optical microscope images of the MHPs fabricated, and photographs of (c) the spin coating system and nTC-coated MHP and (d) pressure cell test system.

1. Introduction

Thermite composites with chemical enthalpy rapidly generate thermal energy and pressure when ignited by the input of external energy. Nanoscale thermite composites (nTCs) have gained wide attention because of their highly exothermic reactions in comparison to macro and microscale thermite composites. They are generally fabricated by mixing pure metal nanoparticles (which act as a fuel) with metal oxide nanoparticles (which act as an oxidizer) in the form of powders [1–11], pellets [12–14], and thin films [15–20]. In various nTC formulations, aluminum (Al), a relatively stable fuel metal, is widely used in combination with copper oxide (CuO) [15, 21–23], which can release the maximum theoretical reaction heat of approximately 3.9 kJ g^{-1} within a fraction of a second. In addition, both Al and CuO employed in nTC-based devices offer the advantages of non-toxicity and abundance. Al and CuO-based nTCs are well known for their relatively high combustion velocity and energy release rate, which are further accelerated at the nanoscale. Recently, the integration of nanoscale Al and CuO-based nTCs into micro-electro-mechanical systems (MEMS) has been made to develop nTCs on a microscale chip (hereafter referred to as nTCs-on-a-chip), which can produce various potential applications in the next generation of very powerful micro initiators, explosives or detonators for both civilian and military purposes [24–27].

To ignite the nTCs, various methods involving mechanical impact, flames, and hot wires have been developed [28–30]. The development of an effective ignition method is a very important requirement for precisely controlling the energetic

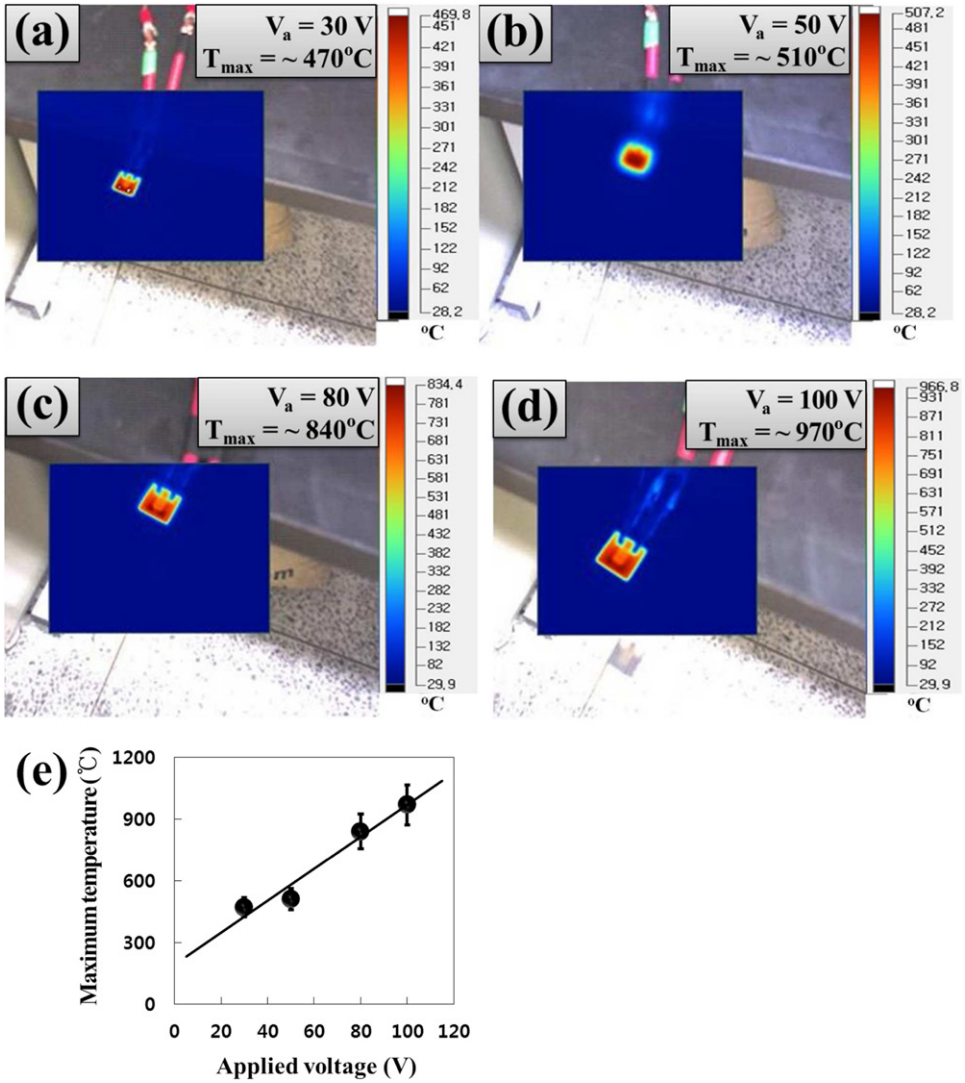

Figure 2. Thermal images of MHPs heated by applying (a) 30 V, (b) 50 V, (c) 80 V, and (d) 100 V. (e) The maximum temperature of the MHP as a function of the applied voltage.

properties (e.g. sensitivity, reaction rate, and energy output) and greatly broadening the potential applications of the nTCs. Among the various ignition methods, an electropyrotechnic igniter activated by minimal electrical energy input is very attractive and is advantageous because of the relative simplicity, easy handling, and compact device realization. The use of traditional electropyrotechnic igniters, which employ various bridge wires, can limit the small-scale integration of multiple nTC-based devices. Recently, microscale electrothermal heaters, which have been fabricated using MEMS-based processing, are being used as explosive initiators for a wide range of civilian and military applications [23, 31–36]. The integration of nTCs-on-a-chip enables the effective supply of high heat for multiscale device-based thermal engineering systems. The performances of such nTCs-on-a-chip have been greatly enhanced; however, various fundamental challenges, such as explosion controllability, ignition reliability, and effective harnessing of heat and pressure, still remain [37–40].

This study reports the design, assembly, and characterization of nTCs-on-a-chip with highly reliable ignition and controllable explosive reactivity. Briefly, a microscale electrothermal initiator platform was fabricated on a silicon substrate to rapidly and effectively ignite nTC-accumulated multilayers. Tuning of the explosive reactivity of the nTCs-on-a-chip was systematically investigated by varying the internal structures of the Al and CuO multilayers accumulated on the surface of the gold (Au) wire-patterned microchips. The energetic properties of a given nTCs-on-a-chip device assembled by this approach have been exhibited in terms of the heat flow, peak explosion time, and pressurization rate when ignited.

2. Experimental methods

The microhotplate (MHP) chips were fabricated by a metal lift-off process, as illustrated schematically in figure 1(a). A photoresist mold ~1.4 μm in thickness (PR; AZ5214, Clariant) was first formed on an oxidized silicon substrate by a standard image reversal (IR) photolithography process. The IR process is useful for producing negatively sloped sidewalls in a PR mold, which makes the subsequent lift-off easier. Hence, the PR was spin-coated on the oxidized silicon

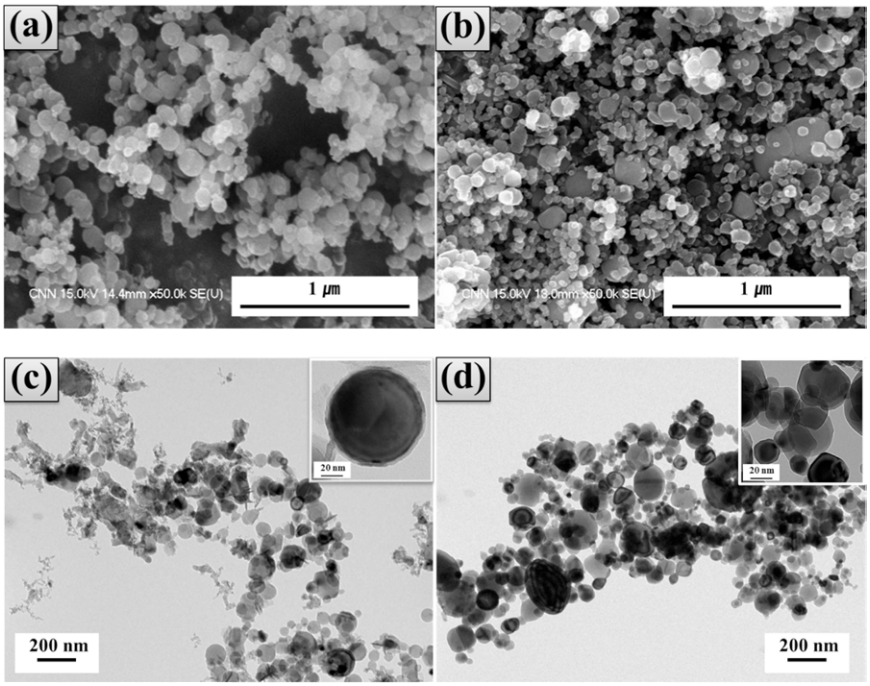

Figure 3. SEM images of (a) Al NPs and (b) CuO NPs. TEM images of (c) Al NPs and (d) CuO NPs.

substrate at 4000 rpm for 35 s and soft-baked on a hotplate at 95 °C for 5 min. The PR layer was then exposed to ultraviolet (UV) radiation with an intensity of ~20 mW cm^{-2} through a photomask using a commercially-available mask aligning system (MDA-400M, Midas System). The UV-exposed region of the PR layer was cross-linked by further baking on a hot-plate at 115 °C for 2.5 min. Subsequently, the processed PR layer was entirely exposed to the UV radiation without a photomask to solubilize the non-cross-linked region. Finally, the PR mold patterns were produced by dissolving the non-cross-linked region using a developer (AZ300 MIF, Clariant). A gold (Au) layer, ~150 nm in thickness, was then deposited on the prepared mold substrate containing a chromium (Cr) adhesion layer (~10 nm in thickness) using a thermal evaporation technique. Finally, serpentine-shaped MHP patterns were defined by selectively removing the unnecessary portions of the deposited Au thin film in an ultrasonic bath containing acetone. Figure 1(b) shows the digital image of the fabricated MHP chip with an effective heating area of ~3 mm × 4 mm. Voltage was applied to the fabricated MHP chips using a variable alternating current (ac) autotransformer (Variac, HCA-2SD20, Han Chang Trans Co. Ltd) capable of supplying an output voltage of up to ~240 V. The temperature distribution of the MHPs applied with various voltages was then measured using an infrared thermal camera (FLK-TI55FT-10/20/54, Fluke).

As mentioned above, Al NPs and CuO NPs were employed as the fuel and oxidizer, respectively. To obtain the Al/CuO NP-accumulated multilayers (MLs), a spin coating process was used because it has the advantages of being simple and providing fast fabrication at atmospheric pressure, as shown in figure 1(c). Al NPs were dispersed in EtOH with an initial concentration of ~10 wt% and CuO NPs were dispersed in EtOH with an initial concentration of ~30 wt%. These two colloidal solutions were sonicated for an hour at ~660 W and 60 Hz. Various Al/CuO MLs were fabricated on the surface of the MHPs installed on the spin coater with a rotation speed of ~1500 rpm. The final thickness of the Al/CuO MLs was fixed at approximately 50 μm and the mixing ratio was fixed of Al : CuO = 30 : 70 wt%. The reason for using the fixed mixing ratio of Al : CuO = 30 : 70 wt% is that it exhibited the best combustion properties among various Al/CuO mixing ratios described elsewhere in our previous studies [6, 7, 12]. The fabricated Al/CuO MLs were then dried in a convection oven at 80 °C for ~30 min. During the spin coating process, the Au electrode was manually masked using an adhesive tape to make effective electrical contact by avoiding particle contamination.

The explosive reactivity of the as-prepared Al/CuO MLs was monitored *in situ* using a high speed camera (Fastcam SA3 120K, Photron) with a frame rate of 15 kHz. A homemade pressure cell tester (PCT) system, as shown in figure 1(d), was employed to measure the pressure trace of the Al/CuO MLs upon the MHP-induced explosion. Briefly, the Al/CuO MLs formed on the MHP surface (i.e. nTCs-on-a-chip) were placed and sealed in a closed pressure cell and ignited by the MHPs supplied with sufficiently high voltage of 100 V via an external ac power supplier for reliable ignition and short response time. The pressure generated by the explosion of the Al/CuO MLs was measured *in situ* by a pressure sensor (Model No. 113A03, PCB Piezotronics) installed in the PCT. The distance between Al/CuO MLs and pressure sensor was approximately 2 cm. The pressure was then amplified by in-line charge amplifiers (Model No. 422E11, PCB Piezotronics) and transformed into an electric signal by a signal conditioner (Model No. 480C02, PCB Piezotronics) with the frequency response of 25 kHz. The final signal was then recorded using a digital oscilloscope (TDS 2012B, Tektronix). To examine

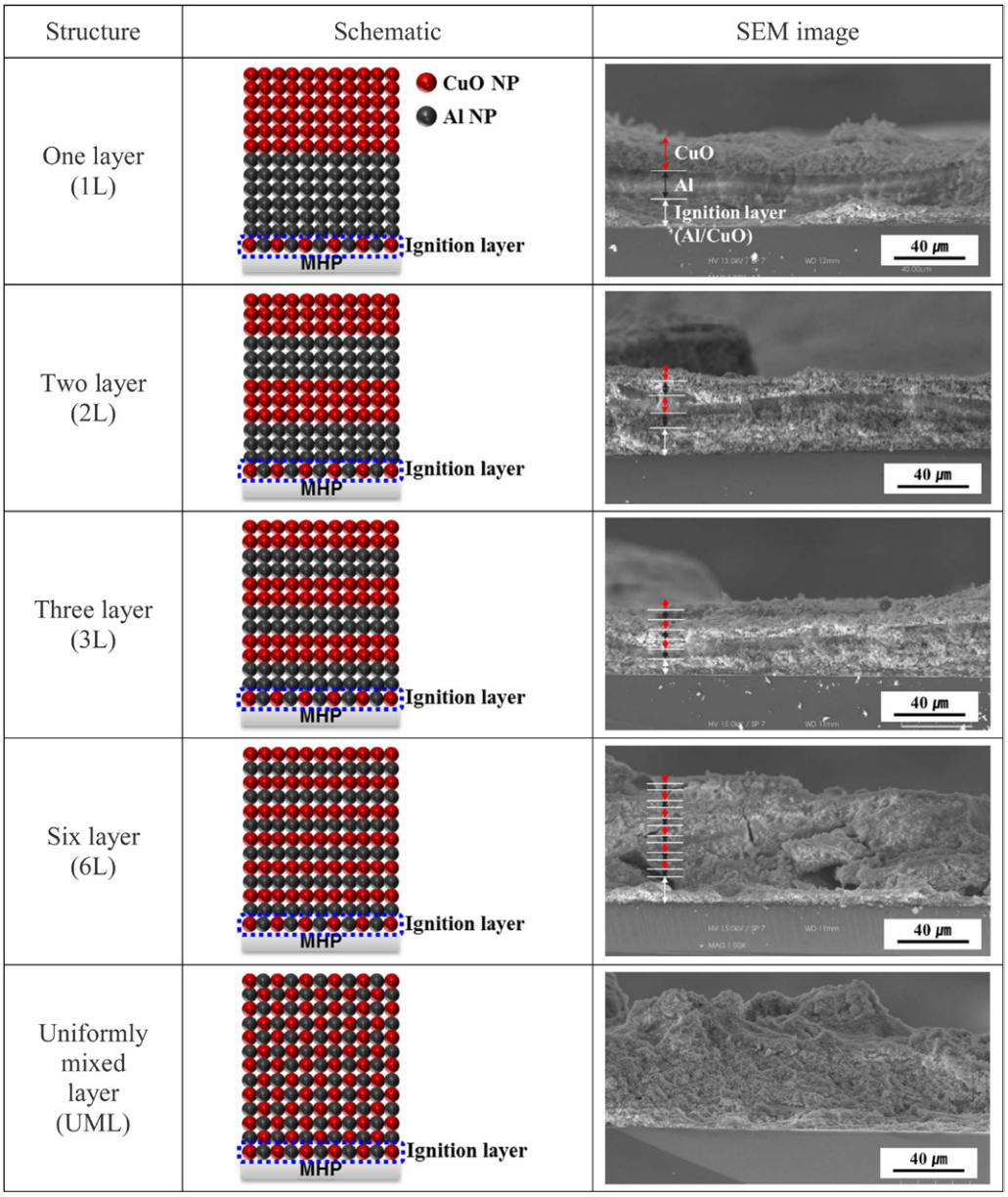

Figure 4. Schematic and cross-sectional SEM images of the various nTC MLs assembled on the surface of silicone oxide substrates.

the heat flow in the various Al/CuO MLs, differential scanning calorimetry (DSC, Setaram, Model No. LABSYS evo) was carried out at temperatures ranging from 30 to 1000 °C at a heating rate of 10 °C min^{-1} under N_2 flow. After obtaining the absolute heat flow data for all different Al/CuO MLs, we simply divided all the data with maximum value of each heat flow curve to relatively compare them in a graph. The total heat energy of Al/CuO MLs was then calculated by integrating each exotherm.

3. Results and discussion

The heating characteristics of the MHPs were measured using a thermal imaging camera. The infrared spectrum was measured at wavelengths ranging from 8 to 14 μm and the measured maximum temperature was up to ~1200 °C. Figures 2(a)–(d) show the thermal images obtained from the as-prepared MHP heated by applying different voltages supplied from an external power supplier. Here the total resistance of the Au electrode fabricated on MHP was measured to be ~ 38 Ω. It was observed that the Au-based electric lines on the surface of the MHP were concentrically heated, as expected. Thermal image analysis revealed that the maximum temperature of the MHPs linearly increased with increase in the applied voltage, as shown in figure 2(e).

Figures 3(a) and (b) show the SEM images of Al and CuO NPs. They were spherical and loosely agglomerated. Figures 3(c) and (d) show the TEM images of Al and CuO NPs. The average diameter of spherical primary Al NPs was 80 nm, and the thickness of the oxide layer was approximately 4 nm as shown in figure 3(c). The average diameter of the primary CuO NPs was approximately 100 nm as shown in figure 3(d).

Figure 4 shows the conceptual schematics and SEM images of the cross-sectional area of various Al/CuO-accumulated

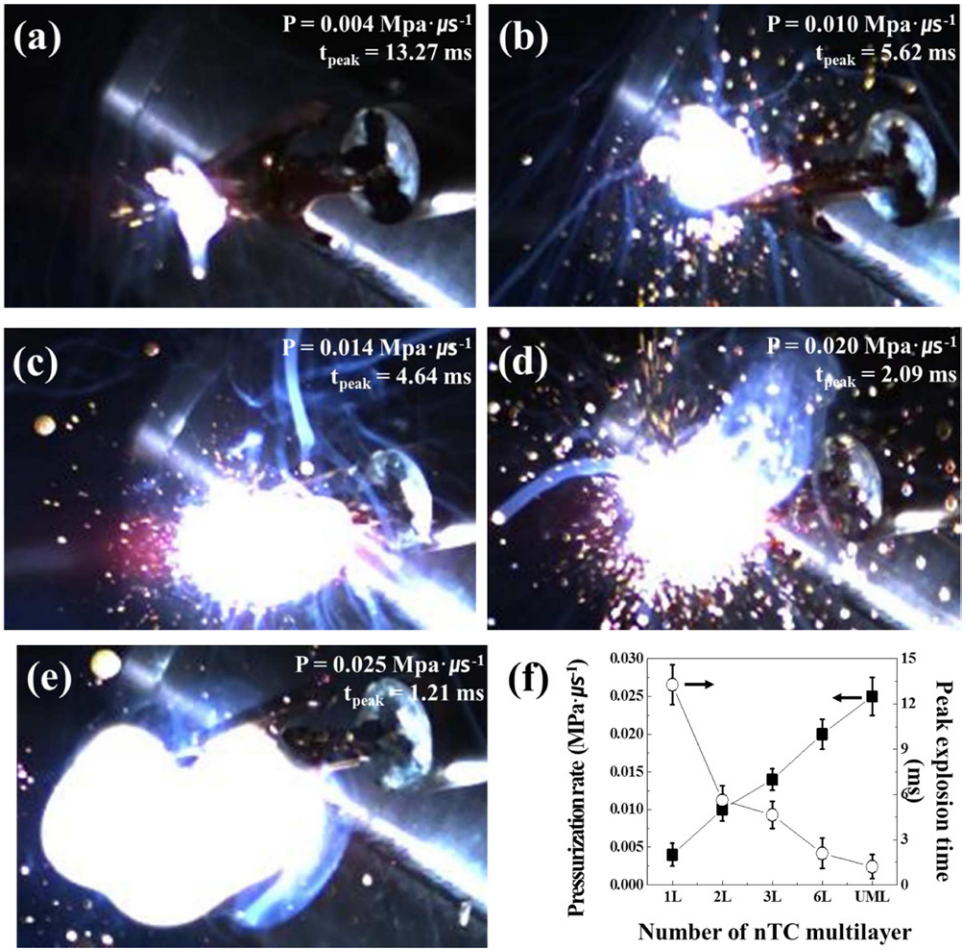

Figure 5. Snapshots and explosive reactivities of various nTC MLs i.e. (a) 1L, (b) 2L, (c) 3L, (d) 6L structures, and (e) UML. (Here, P is the pressurization rate and t_{peak} is the peak explosion time). (f) The pressurization rates and peak explosion times of the various nTC MLs.

MLs assembled by the above-described approach. First, a thin layer composed of uniform Al/CuO NP mixture was placed on the bottom for stable ignition in all cases. Subsequently, an Al layer and CuO layer were placed using a spin coating process. When a single Al layer and a single CuO layer (i.e. Al/CuO layer) were fabricated, the structure is named as a one-layer (1L) structure. Al/CuO/Al/CuO layer structures are termed as two-layer (2L) structures. When a uniform mixture of Al and CuO NPs were used to make a single layer, the structure is termed as a uniformly mixed layer (UML). The final thickness of all the Al/CuO MLs was fixed at approximately 50 μm, which corresponds to a total mass of the Al/CuO composite amounting to approximately 16 mg with the mixing ratio of Al : CuO = 30 : 70 wt%. The thickness of Al/CuO mixture-based initial ignition layer was approximately 15.3 μm. Then the thickness of the Al layer was changed from approximately 15.3 μm for 1 L to 2.5 μm for 6L. The thickness of CuO layer was also changed from approximately 19 μm for 1L to 3.2 μm for 6L. Based on the thickness and total mass of Al/CuO multilayers, the theoretical density of the resulting Al/CuO multilayers was calculated to be approximately 95 %TD. It is also noted that the number of Al and CuO MLs was increased with the intention of increasing the interfacial contact area between Al and CuO NPs and therefore, the explosive reaction can be changed by varying the number of Al/CuO MLs after the MHP ignition. Unlike the presence of a distinct boundary layer between Al/CuO in the different Al/CuO MLs, the UML consisted of homogeneously mixed Al and CuO NPs in a given layer and the NPs were located at close proximity at nanoscale. As shown in figure 4, the cross-sectional SEM images of the Al/CuO MLs taken in the center of substrate showed that the Al and CuO NP-accumulated layers were formed with distinct boundary lines for the various Al/CuO MLs (i.e. 1L, 2L, and 3L structures). The visible division between layers was clear for smaller number of Al/CuO MLs in any location of the chip, while the visible division between Al/CuO MLs was not gradually clear in the case of larger number of Al/CuO MLs (i.e. 6L structure) because each layer was getting thinner. The distinct boundary lines were completely absent in the case of UML because of the initially homogeneous mixing of the Al and CuO NPs.

The ignition and explosive reactivity of the Al/CuO MLs was qualitatively measured using a high speed camera. Figures 5(a)–(e) show the snapshots of the peak explosive reactivity of each Al/CuO ML ignited by the MHP. Initially, several local explosion spots were present in a given nTC's layer and thereafter, the diameter of the explosion-induced

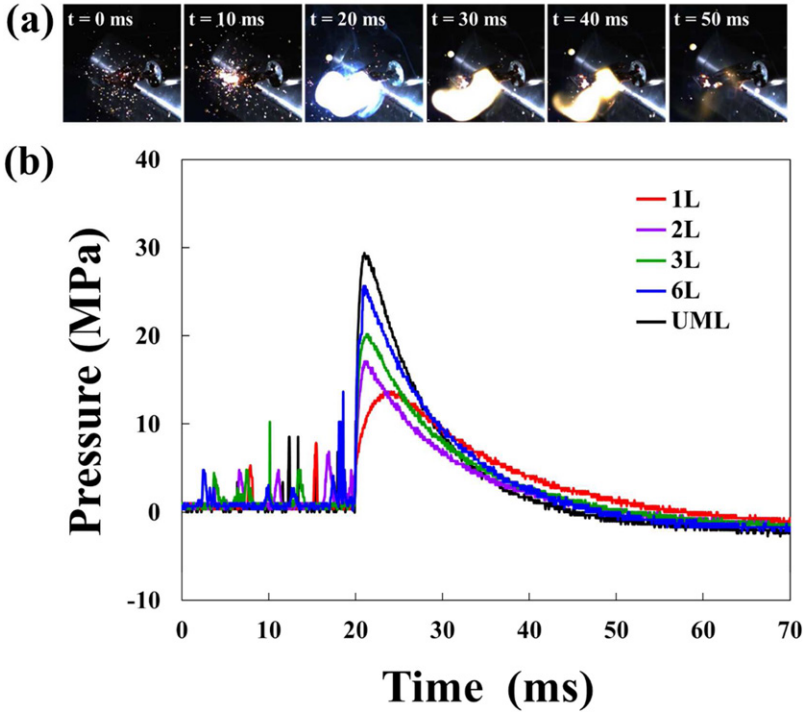

Figure 6. (a) Sequential snapshots of MHP-induced ignition in six layers of Al/CuO-based nTCs and (b) the pressure traces of MHP-ignited nTCs with different Al/CuO accumulating structures.

flash propagation rapidly increased. The peak explosion time (t_{peak}) significantly decreased with increase in the number of the nTC-accumulated MLs because of the enhanced explosive reactivity. The peak explosion time was measured from the initial ignition to the moment of formation of largest explosion-induced flash. With the assistance of a PCT, the pressurization rates of all the Al/CuO MLs were also analyzed. The pressurization rate significantly increased with increase in the number of the Al/CuO MLs and the highest pressurization rate of approximately 0.025 MPa μs^{-1} was achieved in the case of the Al/CuO-based UML. The pressurization rate was determined by dividing the maximum pressure by the rise time (see figure 6). Figure 5(f) shows that the peak explosion time significantly decreased, while the pressurization significantly increased with an increase in the number of the Al/CuO MLs on account of their enhanced explosive reactivity, which occurred because of the increase in the interfacial contact area and the decrease in diffusion distance between Al and CuO NPs. This suggests that the explosive reactivity and peak explosion time of the nTC-on-a-chip can be simply controlled by designing the accumulation structures of the nTC-based MLs.

The representative sequential snapshots obtained in the case of the 6L structure and the pressure traces obtained on ignition of the nTCs-on-a-chip with various nTC MLs measured using the PCT system are presented in figure 6. At the early stages of MHP activation, multiple small pressure peaks were detected at less than 20 ms because of the triggering of non-uniform local explosions in a given Al/CuO ML. A series of snapshots of the Al/CuO MLs shown in figure 6(a) provide evidence for the existence of small local explosions prior to the major pressure rise point. As shown in figure 6(b), major pressure rises occurred in all Al/CuO MLs by rapid propagation of combustion over the entire nTC MLs after ~20 ms of activating the MHP. All the pressure traces were compared under the condition that ignition was occurred at $t = 0$ in all cases. The major pressure peaks were generated at ~20 ms for UML and ~25 ms for 1L, indicating that the time to reach the pressure peak was shorter with an increase in the number of Al/CuO MLs. The relatively small negative pressure phases were also observed at the end of the explosion reactivity of Al/CuO MLs, and this is generally known to occur after the rapid expanding volume of the air blasting phenomenon [41, 42].

DSC analysis was performed to examine the effect of the proximity of the Al and CuO layers on the total heat energy of the nTCs, as shown in figure 7. Free-standing Al/CuO MLs formed on a nitrocellulose (NC) thin film were thermally analyzed using DSC. To obtain free-standing Al/CuO MLs, a NC polymer thin film was intentionally coated on the surface of the MHPs before accumulating the Al/CuO MLs. This is because a NC polymer thin film can be easily detached from the surface of the MHPs. To examine the effect of NC on the Al/CuO MLs, DSC of pure NC, Al/CuO, and NC/Al/CuO were carried out, as shown in figure 7(a). Pure NC showed an exothermic reaction and ignited at approximately 180–220 °C and the Al/CuO mixture thermally ignited at 400–450 °C. The presence of a NC thin film in the Al/CuO matrix was found to ignite the free-standing NC/Al/CuO MLs at lower temperatures and promote total heat energy release. Figure 7(b) shows the results of the DSC analyses of the free-standing Al/CuO MLs with the minimal amount of NC and all the Al/CuO MLs exhibited exothermic reactions and similar ignition temperatures of approximately 180–220 °C. The total

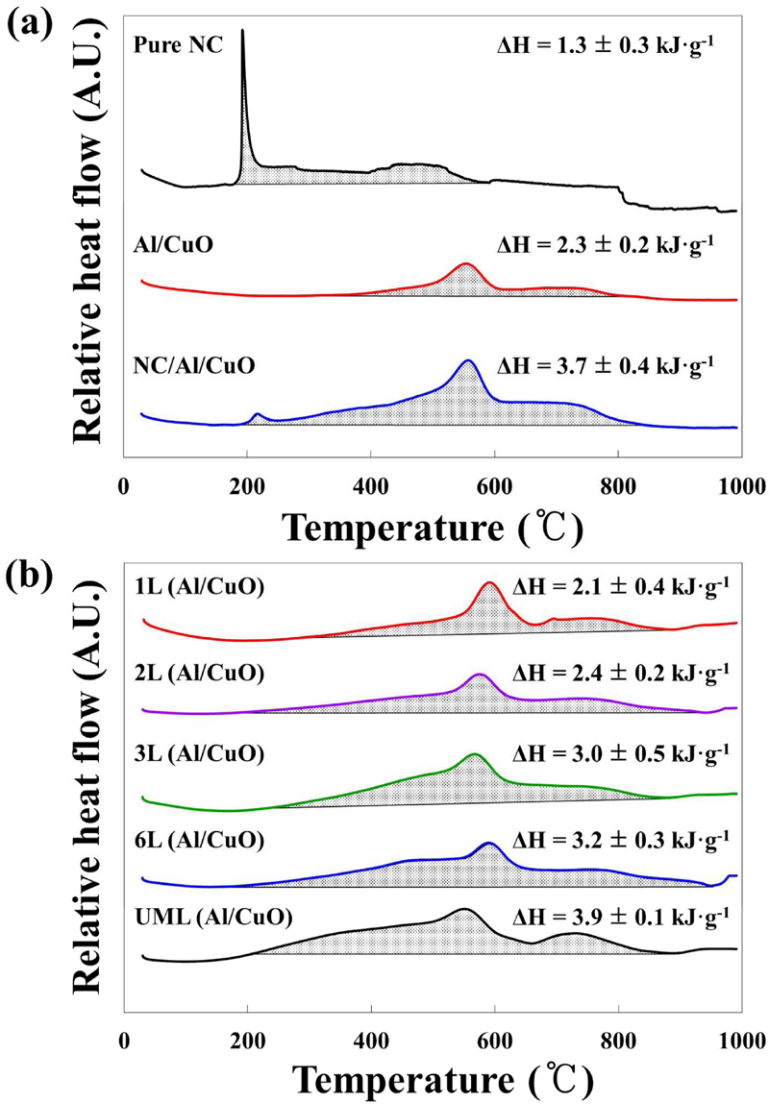

Figure 7. DSC plots of (a) pure NC, Al/CuO NPs, and NC/Al/CuO NPs, and (b) various free-standing Al/CuO MLs with different structures and minimal amount of NC thin films.

heat energy increased with increase in the number of Al/CuO MLs. This suggests that the total energy release was lower for a smaller number of Al/CuO MLs because Al and CuO NPs were not fully reacted, and thus an increase in the interfacial contact area between the Al and CuO NP-accumulated MLs can strongly affect the total heat energy release, because of the improved explosive reaction caused by rapid oxygen supply from the metal oxide layer closely located to the combustion of the fuel metal layer.

4. Conclusions

In this work, various Al/CuO-based nTC MLs were integrated on a silicon oxide substrate with serpentine-shaped Au electrodes to realize nTCs-on-a-chip with controlled explosive reactivity. The nTCs-on-a-chip were fabricated using a combination of MEMS-based processes and simple nanofabrication methods, which enabled the building of potentially compact and small-scale devices. Various thin films composed of Al/CuO-based nTCs coated with a fixed thickness of ~50 μm were ignited and rapidly exploded when a voltage was supplied to the MHPs. The nTCs-on-a-chip assembled by the approach demonstrated the capability to be ignited with a high reliability of a firing maximum current range of approximately 8 A with a compliance of 100 V, and a relatively fast response time ranging from 2 to 20 ms. In addition, the device can produce pressurization rates ranging from 0.004 to 0.025 MPa μs^{-1} and controlled heat flows of approximately 2.0–3.8 kJ g^{-1} were achieved by simply changing the accumulating structure of the Al/CuO MLs. The explosive reactivity of the nTCs-on-a-chip was found to enhance by increasing the interfacial contact area between the Al and CuO NP-accumulated ML with a fixed total thickness, which can provide rapidly oxygen from the metal oxide layer closely located to the combustion of the fuel metal layer. The nTCs-on-a-chip realized by the approach detailed in this report exhibit controlled explosive reactivity and fast response time and can potentially be used in civilian and military applications.

Acknowledgments

This research was supported by the Civil & Military Technology Cooperation Program through the National Research Foundation of Korea (NRF) funded by the Ministry of Science, ICT & Future Planning (No 2013M3C1A9055407).

References

[1] Munir Z R 1988 Synthesis of high-temperature materials by self-propagating combustion methods *Am. Ceram. Soc. Bull.* **67** 342–9
[2] Valliappan S, Swiatkiewicz J and Puszynski J A 2005 Reactivity of aluminum nanopowders with metal oxides *Powder Technol.* **156** 164–9
[3] Prakash A, McCormick A V and Zachariah M R 2004 Aero-sol−gel synthesis of nanoporous iron-oxide particles: a potential oxidizer for nanoenergetic materials *Chem. Mater.* **16** 1466–71
[4] Mehendale B, Shende R, Subramanian S, Gangopadhyay S, Redner P, Kapoor D and Nicolich S 2006 Nanoenergetic composite of mesoporous iron oxide and aluminum nanoparticles *J. Energy Mater.* **24** 341–60
[5] Prakash A, McCormick A V and Zachariah M R 2005 Tuning the reactivity of energetic nanoparticles by creation of a core − shell nanostructure *Nano Lett.* **5** 1357–60
[6] Ahn J Y, Kim W D, Cho K, Lee D G and Kim S H 2011 Effect of metal oxide nanostructures on the explosive property of metastable intermolecular composite particles *Powder Technol.* **211** 65–71
[7] Ahn J Y, Kim W D, Kim J H, Kim J H, Lee J K, Kim J M and Kim S H 2011 Gas-phase synthesis of bimetallic oxide nanoparticles with designed elemental compositions for controlling the explosive reactivity of nanoenergetic materials *J. Nanomater.* **2011** 216709
[8] Sullivan K T, Kuntz J K and Gash A E 2012 Electrophoretic deposition and mechanistic studies of nano-Al/CuO thermites *J. Appl. Phys.* **112** 024316
[9] Son F S, Asay B W, Foley T J, Yetter R A, Wu M H and Risha G A 2007 Combustion of nanoscale Al/MoO_3 thermite in microchannels *J. Propul. Power* **23** 715–21
[10] Séverac F, Alphones P, Estève A, Bancaud A and Rossi C 2012 High-energy Al/CuO nanocomposites obtained by DNA-directed assembly *Adv. Funct. Mater.* **22** 323–9
[11] Apperson S, Shende R V, Subramanian S, Tappmeyer D, Gangopadhyay S, Chen Z, Gangopadhyay K, Redner P, Nicholich S and Kapoor D 2007 Generation of fast propagating combustion and shock waves with copper oxide/aluminum nanothermite composites *Appl. Phys. Lett.* **91** 243109
[12] Ahn J Y, Kim J H, Kim J M, Lee D W, Park J K, Lee D G and Kim S H 2013 Combustion characteristics of high-energy Al/CuO composite powders: The role of oxidizer structure and pellet density *Powder Technol.* **241** 67–73
[13] Guidotti R A, Odinek J and Reinhardt F W 2006 Characterization of Fe/$KClO_4$ heat powders and pellet *J. Energy Mater.* **24** 271–305
[14] Granier J J and Pantoya M L 2004 Ignition and combustion behaviors of nanocomposite Al/MoO_3 *Mater. Res. Soc. Symp. Proc.* **800** AA5.3.1
[15] Blobaum K J, Feiss M E, Lawrence J M P and Weihs T P 2003 Deposition and characterization of a self-propagating CuO_x/Al thermite reaction in a multilayer foil geometry *J. Appl. Phys.* **94** 2915–22
[16] Blobaum K J, Wanger A J, Plitzko J M, Van Heerden D, Fairbrother D H and Weihs T P 2003 Investigating the reaction path and growth kinetics in CuO_x/Al multilayer foils *J. Appl. Phys.* **94** 2923–9
[17] Petrantoni M, Rossi C, Salvagnac L, Conedera V, Esteve A, Tenailleau C, Alphonse P and Chabal Y J 2010 Multilayered Al/CuO thermite formation by reactive magnetron sputtering: nano versus micro *J. Appl. Phys.* **108** 084323
[18] Manesh N A, Basu S and Kumar R 2010 Experimental flame speed in multi-layered nano-energetic materials *Combust. Flame* **157** 476–80
[19] Marín L, Nanayakkara C E, Veyan J, Warot-Fonrose B, Joulie S, Estève A, Tenailleau C, Chabal Y J and Rossi C 2015 Enhancing the reactivity of Al/CuO nanolaminates by Cu incorporation at the interfaces *ACS Appl. Mater. Interf.* **7** 11713–8
[20] Bahrami M, Taton G, Conédéra V, Salvagnac L, Tenailleau C, Alphones P and Rossi C 2014 Magnetron sputtered Al–CuO nanolaminates: effect of stoichiometry and layers thickness on energy releases and burning rate *Propell. Explos. Pyrot.* **39** 365–73
[21] Shen J, Qiao Z, Wang J, Zhang K, Li R, Nie F and Yang G 2014 Pressure loss and compensation in the combustion process of Al–CuO nanoenergetics on a microheater chip *Combust. Flame* **161** 2975–81
[22] Zhu P, Shen R, Ye Y, Fu S and Li D 2013 Characterization of Al/CuO nanoenergetic multilayer films integrated with semiconductor bridge for initiator applications *J. Appl. Phys.* **113** 184505
[23] Taton G, Lagrange D, Conedera V, Renaud L and Rossi C 2013 Micro-chip initiator realized by integrating Al/CuO multilayer nanothermite on polymeric membrane *J. Micromech. Microeng.* **23** 105009
[24] Zhang K, Rossi C, Petrantoni M and Mauran N A 2008 Nano initiator realized by integrating Al/CuO-based nanoenergetic materials with a Au/Pt/Cr microheater *J. Microelectromech. Syst.* **17** 832–6
[25] Guidotti R A and Masset P 2006 Thermally activated ('thermal') battery technology: I. An overview *J. Power Sources* **161** 1443–9
[26] Son S F 2003 Performance and characterization of nanoenergetic materials at Los Alamos *Mater. Res. Soc. Symp. Proc.* **800** AA5.2
[27] Cheng J L, Hng H H, Lee Y W, Du S W and Thadhani N N 2010 Kinetic study of thermal- and impact-initiated reactions in Al–Fe_2O_3 nanothermite *Combust. Flame* **157** 2241–9
[28] Granier J J and Pantoya M L 2004 Laser ignition of nanocomposite thermites *Combust. Flame* **138** 373–83
[29] Zhou X, Torabi M, Lu J, Shen R and Zhang K 2014 Nanostructured energetic composites: synthesis, ignition/combustion modeling, and applications *ACS Appl. Mater. Interface* **6** 3058–74
[30] Rossi C, Zhang K, Estève D, Alphonse P, Taihades P and Vahlas C 2007 Nanoenergetic materials for MEMS: a review *J. Microelectromech. Syst.* **16** 919–31
[31] Rossi C, Larangot B, Lagrange D and Chaalane A 2005 Final characterizations of MEMS-based pyrotechnical microthrusters *Sensors Actuators* A **121** 508–14
[32] Zhang K, Chou S K and Ang S S 2007 Investigation on the ignition of a MEMS solid propellant microthruster before propellant combustion *J. Micromech. Microeng.* **17** 322–32
[33] Staley C S, Morris C J, Thiruvengadathan R, Apperson S J, Gangopadhyay K and Gangopadhyay S 2011 Silicon-based bridge wire micro-chip initiators for bismuth oxide-aluminum nanothermite *J. Micromech. Microeng.* **21** 115015
[34] Wang J, Zhang W, Wang L, Shen R, Xu X, Ye J, Chao Y 2014 Novel approach to the preparation of organic energetic film for microelectromechanical systems and microactuator applications *ACS Appl. Mater. Interf.* **6** 10992–6

[35] Piekiel N W, Morris C J, Currano L J, Lunking D M, Isaacson B and Churaman W A 2014 Enhancement of on-chip combustion via nanoporous silicon microchannels *Combust. Flame* **161** 1417–24
[36] Glavier L, Taton G, Ducéré J, Baijot V, Pinon S, Calais T, Estève A, Rouhani M D and Rossi C 2015 Nanoenergetics as pressure generator for nontoxic impact primers: comparison of Al/Bi_2O_3, Al/CuO, Al/MoO_3 nanothermites and Al/PTFE *Combust. Flame* **162** 1813–20
[37] Zhang W, Peng H, Gao X, Ye J, Zhang Z and Chao Y 2012 An *in situ* chemical reaction approach to synthesize zinc picrate energetic thin film upon zinc oxide nanowires array *Surf. Interf. Anal.* **44** 1203–8
[38] Zhang D, Li X, Qin B, Lai C and Guo X 2014 Electrophoretic deposition and characterization of nano-Al/Fe_2O_3 thermites *Mater. Lett.* **120** 224–7
[39] Manesh N A, Basu S and Kumar R 2011 Modeling of a reacting nanofilm on a composite substrate *Energy* **36** 1688–97
[40] Zhang G, Weeks B L and Holtz M 2011 Application of dynamic scaling to the surface properties of organic thin films: energetic materials *Surf. Sci.* **605** 463–7
[41] Smith P D and Hetherington J G 1994 *Blast and Ballistic Loading of Structure* (Oxford: Butterworth-Heinemann) p 336
[42] Kinney G and Graham K 1985 *Explosive Shocks in Air* (New York: Springer) p 137